International Journal for Parasitology: Drugs and Drug Resistance 3 (2013) 93–101

Contents lists available at SciVerse ScienceDirect

International Journal for Parasitology: Drugs and Drug Resistance

journal homepage: www.elsevier.com/locate/ijpddr

Identification of mutations in TgMAPK1 of *Toxoplasma gondii* conferring resistance to 1NM-PP1 ☆

Tatsuki Sugi [a], Kyousuke Kobayashi [b], Hitoshi Takemae [a], Haiyan Gong [a], Akiko Ishiwa [a], Fumi Murakoshi [a], Frances C. Recuenco [a], Tatsuya Iwanaga [a], Taisuke Horimoto [a], Hiroomi Akashi [a], Kentaro Kato [a,c,*]

[a] Department of Veterinary Microbiology, Graduate School of Agricultural and Life Sciences, The University of Tokyo, 1-1-1 Yayoi, Bunkyo-ku, Tokyo 113-8657, Japan
[b] Department of Host-Parasite Interaction, Division of Microbiology and Immunology, Institute of Medical Science, The University of Tokyo, 4-6-1 Shirokanedai, Minato-ku, Tokyo 108-8639, Japan
[c] National Research Center for Protozoan Diseases, Obihiro University of Agriculture and Veterinary Medicine, Inada-cho, Obihiro, Hokkaido 080-8555, Japan

ARTICLE INFO

Article history:
Received 21 December 2012
Received in revised form 17 April 2013
Accepted 22 April 2013
Available online 18 May 2013

Keywords:
1NM-PP1
Bumped kinase inhibitor
Drug resistance
TgMAPK1
Toxoplasma gondii

ABSTRACT

Toxoplasma gondii is an important food and waterborne pathogen that causes severe disease in immunocompromised patients. Bumped kinase inhibitors (BKIs) have an antiparasitic effect on *T. gondii* tachyzoite growth by targeting *T. gondii* calmodulin-domain protein kinase 1 (TgCDPK1). To identify mutations that confer resistance to BKIs, chemical mutagenesis was performed, followed by selection in media containing either 250 or 1000 nM 1NM-PP1. Whole-genome sequence analysis of resistant clones revealed single nucleotide mutations in *T. gondii* mitogen-activated protein kinase 1 (TgMAPK1) at amino acids 162 (L162Q) and 171 (I171N). Plasmid constructs having the TgMAPK1 L162Q mutant sequence successfully replaced native TgMAPK1 genome locus in the presence of 1000 nM 1NM-PP1. The inhibitory effect of 1NM-PP1 on cell division observed in the parent clone was decreased in 1NM-PP1-resistant clones; however, effects on parasite invasion and calcium-induced egress were similar in both parent and resistant clones. A plasmid construct expressing the full length TgMAPK1 splicing isoform with L162Q mutation successfully complemented TgMAPK1 function in the pressure of 250 nM 1NM-PP1 in plaque assay. 1NM-PP1-resistant clones showed resistance to other BKIs (3MB-PP1 and 3BrB-PP1) with different levels. Here we identify TgMAPK1 as a novel target for 1NM-PP1 activity. This inhibitory effect is mediated through inhibition of tachyzoite cell division, and can be overcome through mutations at multiple residues in TgMAPK1.

1. Introduction

Toxoplasma gondii is an obligate intracellular parasite of the phylum Apicomplexa, which includes the causative pathogens of toxoplasmosis, malaria, and cryptosporidiosis. Bumped kinase inhibitors (BKIs) have been shown to inhibit tachyzoite growth in *T. gondii* (Lourido et al., 2010; Ojo et al., 2010; Sugi et al., 2010; Larson et al., 2012), *Cryptosporidium parvum* infection (Murphy et al., 2010) and transmission of the malaria parasite from humans to mosquitoes (Ojo et al., 2012). BKIs are protein kinase inhibitor analogs which primarily affect analog-sensitive protein kinases containing a small amino acid at the gatekeeper position (Shokat and Velleca, 2002). Gatekeeper amino acids are found at the entrance of the protein kinase ATP-binding pocket; the size and shape of this amino acid greatly affects the susceptibility of protein kinases to kinase inhibitor analogs (Shokat and Velleca, 2002). Analog-sensitive protein kinases are rarely encoded in mammalian genomes.

The genomes of *Toxoplasma*, *Neospora*, and *Cryptosporidium* encode for calmodulin-domain protein kinase 1 (CDPK1) homologs (TGME49_101440, NCLIV_011980, and cgd3_920 in the EuPathDB http://eupathdb.org/eupathdb/) containing a glycine at the gatekeeper amino acid position. Both TgCDPK1 (Lourido et al., 2010; Murphy et al., 2010; Sugi et al., 2010; Larson et al., 2012) and CpCDPK1 (Murphy et al., 2010) have been confirmed as the primary targets of BKIs, however the *T. gondii* genome encodes for other analog-sensitive protein kinases containing a small amino acid such as Ala, Ser and Thr at the gatekeeper position, suggesting the possibility of multiple targets (Sugi et al., 2010). BKIs therefore represent a promising new class of antiparasitic compounds.

To predict the frequency at which BKI-resistant parasites may arise, identification of mutations conferring resistance to these inhibitors is required. Resistance to BKIs is predicted to occur

* Corresponding author at: Department of Veterinary Microbiology, Graduate School of Agricultural and Life Sciences, The University of Tokyo, 1-1-1 Yayoi, Bunkyo-ku, Tokyo 113-8657, Japan. Tel.: +81 3 5841 5398; fax: +81 3 5841 8184.
E-mail address: akkato@mail.ecc.u-tokyo.ac.jp (K. Kato).

2211-3207/$ - see front matter © 2013 The Authors. Published by Elsevier Ltd. All rights reserved.
http://dx.doi.org/10.1016/j.ijpddr.2013.04.001

through mutation of both the gatekeeper residue of the target protein kinases, as well as other amino acids affecting the affinity of protein kinase inhibitors to their respective targets. Mutation of the gatekeeper residue of TgCDPK1 from wild-type (WT) glycine to methionine, which contains a larger side chain than that of glycine, has been shown to confer resistance in transfected parasites (Lourido et al., 2010; Murphy et al., 2010; Sugi et al., 2010; Larson et al., 2012). This effect is not limited to gatekeeper residues though, as mutation at other sites within the protein kinase domain have been shown to confer resistance to ATP pocket binding inhibitors such as imatinib (Weisberg and Griffin, 2000) and nilotinib (Ray et al., 2007). Accordingly, we chose to screen for all mutations conferring resistance to BKIs, including those not found at the gatekeeper residue, using randomly mutated parasites. This strategy of using chemically mutated parasite lines, followed by whole-genome sequencing, has recently been validated in *T. gondii* as a means of identifying relevant mutations (Farrell et al., 2012).

In the present study, we used the protein kinase inhibitor analog 1NM-PP1 to select for chemically mutated resistant parasite clones in *T. gondii* type II strain PLK/DUAL (Unno et al., 2009). To fully characterize the inhibitory effects of BKIs, replication inhibition during bradyzoite differentiation, along with effects of inhibitors on parasite stress responses, should be considered. To observe such inhibitory effects across different stages of the parasite life cycle, we employed a PLK/DUAL strain. This strain was derived from a type II PLK strain, and has the capacity for both tachyzoite and bradyzoite differentiation (Unno et al., 2009). Whole-genome sequencing was used to identify mutations in protein kinases which conferred resistance to BKIs. We then analyzed the effect of these mutations on cell invasion, host cell egress, and cell division to better understand the mechanism of resistance.

2. Materials and methods

2.1. Tested reagents

1NM-PP1 was purchased from Merck KGaA (Darmstadt, Germany). 3BrB-PP1 and 3MB-PP1 were purchased from Toronto Research Chemicals (Ontario, Canada).

2.2. Parasite cultures

Tachyzoites of the *T. gondii* PLK/DUAL (Unno et al., 2009) strain (kindly provided by Dr. Y. Takashima, Gifu University, Gifu, Japan) and PLK/hxgprt$^-$ strain (Roos et al., 1994) (NIH AIDS Reagent Program, Division of AIDS, NIAID, NIH #2860) were used in this study. Parasites were maintained in monolayers of Vero cells cultured in Dulbecco's modified Eagle's medium (DMEM) (Nissui, Tokyo, Japan) containing 1% fetal calf serum (FCS) and 2 mM L-glutamine, streptomycin, and penicillin. Host Vero cells were passaged in the same medium containing 5% FCS. For assays, tested reagents or a DMSO control solvent were added to the same medium with 1% FCS (infection medium).

2.3. Chemical mutagenesis

Random mutagenesis was introduced using *N*-ethyl-*N*-nitrosourea (ENU) (Sigma-Aldrich, St. Louis, MO, USA) as previously described (Nagamune et al., 2007). PLK/DUAL tachyzoites (5.0×10^7) were inoculated onto Vero cells cultured in T75 flasks. At 2 h post inoculation (hpi), parasites were exposed to ENU (500 μg/mL) for 1 h in serum-free culture medium, then washed three times in infection medium. They were then incubated at 37 °C for an additional 24 h, followed by 1NM-PP1 selection. Mutated parasites were selected using 1NM-PP1 at either 250 or 1000 nM for 3 weeks with medium changes every 2 days. Parasites were passaged to a new host monolayer every 7 days with host cells ruptured by passage through a 25-G needle to remove uninfected cells. Resistant parasites were cloned by limiting dilution and designated as either PLK/DUAL res.1 for 250 nM selection or PLK/DUAL res.2 for 1000 nM selection.

2.4. Sequence analysis and structure prediction of mutated TgMAPK1

The peptide sequence of the TgMAPK1 (GenBank: AY684849) protein kinase domain (from amino acid 81 to 532) was aligned with HsErk5 (GenBank: NP_002740.2), and CpCDPK1 (GenBank: 3NCG_A). Subdomain prediction was performed according to the method of Hanks and Hunter (1995). ATP-binding sites were predicted by NCBI conserved domain search (Marchler-Bauer et al., 2011). 1NM-PP1-binding sites were predicted from the structure of 1NM-PP1 bound CpCDPK1 (Murphy et al., 2010) (PDB: 3NCG). For homology modeling, the TgMAPK1 protein kinase domain (amino acid residues 81–532) was used for structure calculation by SWISS-MODEL automated mode (Arnold et al., 2006) using the crystal structure of *Homo sapiens* MAPK7 (HsErk5) bound with inhibitor (PDB: 4B99) as a template. The predicted structure was superimposed over the 1NM-PP1-bound CpCDPK1 structure (PDB: 3NCG) using UCSF Chimera (Pettersen et al., 2004).

2.5. Assay for BKIs inhibition of parasite growth

The growth of PLK/DUAL and resistant clones was evaluated using the DsRed-Express reporter gene expressed under the control of a SAG1 promoter. Parasites were pre-incubated with various concentrations of 1NM-PP1, 3BrB-PP1, and 3MB-PP1 or the control solvent (DMSO) for 10 min at room temperature. 5000 parasites per well were inoculated on full Vero cell monolayers in 48-well plates, and cultured with the tested reagent for 6 days. After incubation, media were aspirated and cells lysed using phosphate buffered saline (PBS) containing 0.5% sodium dodecyl sulfate to reduce background fluorescence. Cell lysates were moved to 96 well plates and measured using an SH-9000 fluorimeter (Corona Electronic, Ibaraki, Japan) with an excitation wave length of 540 nm and an emission wave length of 590 nm. Background fluorescence intensities were detected using mock infected wells, and subtracted from the values of all wells.

2.6. Whole-genome sequencing and single nucleotide variants (SNV) identification

SOLiD sequencing libraries were generated from genomic DNA of PLK/DUAL, PLK/DUAL res.1, and PLK/DUAL res.2 strains. Libraries were sequenced using a 5500xl SOLiD system (Life Technologies, Carlsbad, CA) according to the manufacturer's instructions using 75-bp single-end reads. Sequencing data has been submitted to DDBJ (DDBJ: DRA000618). Reads were mapped to the *T. gondii* ME49 genome (ToxoDB http://toxodb.org/version 2008_07_23) using alignment software BWA (Li et al., 2009). SNVs were called with SAMTOOLS (Li et al., 2009) and filtered using a minimal coverage of 10, a maximum coverage of 100, and an alternative bases positive rate of >80%. The average depth was calculated with a 100-kbp window. SNVs were further filtered using a predicted gene model in ToxoDB version 7.2.

2.7. Transgenic parasites

Approximately 2-kbp sequences of TgMAPK1 adjacent to the mutated sites, and lacking a promoter and start codon were amplified from genomic DNA of parent and resistant clones. Primers TgMAPK1_F1 and TgMAPK1cla1_R2 (Supplemental Table 1) were used to generate the first-half fragment, and primers TgMAPK1_R1

and TgMAPK1cla1_F2 (Supplemental Table 1) were used to generate the second-half fragment. The first-half fragment was digested with *Eco*RI and *Cla*I, while the second-half fragment was digested with *Cla*I and *Sma*I. The two fragments were inserted into the *Eco*RI and *Sma*I sites of pBluescript KS(−) to produce a *Cla*I site without affecting the TgMAPK1 coding sequence. Plasmids containing sequences from PLK/DUAL, PLK/DUAL res.1, and PLK/DUAL res.2 were designated pTgMAPK1_WT, pTgMAPK1_LQ, and pTgMAPK1_IN, respectively. Twenty micrograms of each plasmid was transfected, either separately or in combination, into 1.8×10^7 freshly purified PLK/DUAL cells with Nucleofection™ and basic parasite Nucleofector® kit 1, using Nucleofector® II device program U-33 (Lonza, Basel, Switzerland). Following transfection, cells were incubated at 37 °C for 24 h, and treated with 1000 nM 1NM-PP1. After 3 weeks of selection, genomic DNA from parasites was purified using a QIAamp DNA mini kit (QIAGEN) according to the manufacturer's instructions.

PCR of the genomic locus containing TGME49_112570 was performed using KOD Fx Neo (TOYOBO, Osaka, Japan) and 35-mer primers genomic_Locus_primer_F and genomic_Locus_primer_R (Supplemental Table 1) with step-down PCR under the following conditions: initial denaturation at 94 °C for 2 min, 5 cycles of 98 °C for 10 s and 74 °C for 10 min, 5 cycles of 98 °C for 10 s and 72 °C for 10 min, 5 cycles of 98 °C for 10 s and 70 °C for 10 min, and 25 cycles of 98 °C for 10 s and 68 °C for 10 min, followed by a final extension at 68 °C for 10 min. Amplified PCR products were used for the restriction enzyme cut assay. Sequence analysis of mutation sites was performed using primers Mutation_screen_F and Mutation_screen_R (Supplemental Table 1). Resistant parasites were cloned by limiting dilution; sequence analysis was performed as described above.

For the functional expression of TgMAPK1, a TgMAPK1 splicing variant was investigated. Gene modeling in ToxoDB suggests the presence of eight exons in TgMAPK1, and is supported by RNA-seq data demonstrating mRNA containing eight exons. Splicing at intron 7 was confirmed by RT-PCR using primers Splicing_confirm_F and Splicing_confirm_R (Supplemental Table 1).

Because of the long mRNA sequence, we could not amplify the TgMAPK1 full length isoform in a single PCR reaction. Accordingly, we divided the gene into two parts; we amplified the 1st half from total RNA using primers 1st_half_F and 1st_half_R (Supplemental Table 1), the 2nd half using primers 2nd_half_F and 2nd_half_R (Supplemental Table 1). The TgMAPK1 full length isoform was then amplified by overlapping PCR using the 1st half and 2nd half PCR products as templates with primers 1st_half_F and 2nd_half_R. This full-length isoform was then cut using *Eco*RI and *Eco*RV restriction enzymes, and inserted into the *Eco*RI and *Eco*RV site of pMini.ht.3xFLAG (Sugi et al., 2010). The resulting plasmid expressed TgMAPK1 tagged with a C-terminal 3xFLAG driven by a GRA1 promoter. Plasmids containing the WT sequence and L162Q mutation were designated pTgMAPK1-FLAG and TgMAPK1^{L162Q}-FLAG, respectively. As a control, GFP was amplified from the pMini.GFP.ht (Arrizabalaga et al., 2004) using primers GFP_F and GFP_R (Supplemental Table 1), and inserted into the *Bgl*II and *Eco*RV site of pMini.ht.3xFLAG to express C-terminal 3xFLAG-tagged GFP. Plasmids were transfected into *T. gondii* strain PLK/hxgprt$^-$, selected with 25 μg Mycophenolic acid and 50 μg Xanthine, as described (Arrizabalaga et al., 2004), and cloned by limiting dilution. Cloned parasites stably expressing WT and L162Q mutated TgMAPK1 or GFP tagged with 3xFLAG were designated to PLK/TgMAPK1-FLAG, PLK/TgMAPK1^{L162Q}-FLAG and PLK/GFP-FLAG, respectively.

2.8. Invasion assay

Invasion assays were performed as described previously (Sugi et al., 2010). Briefly, freshly harvested and purified parasites were incubated in the tested reagent for 10 min at room temperature and inoculated onto a monolayer of Vero cells for 30 min at 37 °C with 500 nM 1NM-PP1 or with DMSO. Following invasion, cells were washed three times with ice cold PBS, and extracellular parasites stained with anti-SAG1 monoclonal antibodies (1:1000 dilution) [TP3] (Santa Cruz Biotechnology, Santa Cruz, CA) in PBS containing 2% FCS for 30 min. After staining, the cells were washed three times with PBS containing 2% FCS, fixed with 4% paraformaldehyde in PBS, and stained with ALEXA 633 conjugated goat anti-mouse antibodies. Stained cells were visualized with a Zeiss LSM510 system. Microscopic fields were chosen at random; extracellular parasites were detected using anti-SAG1 antibodies and total parasites detected by DsRed-Express.

2.9. Calcium-induced egress assay

A calcium-induced egress assay was performed as described (Lourido et al., 2010). Briefly, purified parasites were inoculated onto a monolayer of Vero cells and allowed to invade for 2 h. At 2 hpi, the cells were washed with PBS to remove non-invaded parasites and incubated in infection medium overnight. At 30 hpi, the media were changed to media containing the reagent of interest and incubated for 10 min at room temperature. Calcium was induced by the addition of media containing 5 μM A23187 along with the reagent of interest. Cells were incubated at 37 °C for 5 min, and egress stopped by addition of 4% paraformaldehyde in PBS for 10 min on ice.

2.10. Cell division assay

Cell division assays were performed as described elsewhere (Kurokawa et al., 2011). Briefly, parasites were inoculated into an eight-well chamber slide containing Vero cells grown in a monolayer, and incubated at 37 °C for 1 h. Following incubation, cells were washed with warm infection medium three times to remove non-invaded parasites, followed by incubation in infection medium with 250 nM 1NM-PP1 or DMSO. After incubation for 12 and 24 h, the cells were fixed with 4% paraformaldehyde in PBS for 10 min at room temperature, washed three times with PBS, dried at room temperature, and mounted with Fluorescence Mounting Medium (Dako, Glostrup, Denmark). Cells were observed by fluorescence microscopy (Olympas, Tokyo, Japan). Microscopic fields were chosen at random to count parasitophorous vacuoles. Average numbers of tachyzoites per vacuole were calculated.

3. Results

3.1. Generation of 1NM-PP1-resistant parasites by N-ethyl-N-nitrosourea (ENU)-induced random mutagenesis

To identify mutations conferring resistance to BKI 1NM-PP1, *T. gondii* strain PLK/DUAL was mutagenized by treatment with ENU, and selected with either 250 or 1000 nM 1NM-PP1. Two independent 1NM-PP1-resistant parasite clones were generated, designated PLK/DUAL res.1 and PLK/DUAL res.2. Sensitivity of resistant clones to 1NM-PP1 was determined using a tachyzoite growth assay. IC_{50} values for clones PLK/DUAL res.1 and PLK/DUAL res.2 were 290 and 210 nM, respectively, compared to 84 nM for parental strain PLK/DUAL (Fig. 1A). The effect of 1NM-PP1 treatment was reduced in resistant clones, especially at 250 and 500 nM (Fig. 1A).

3.2. Identification of SNPs in the resistant clones

To identify mutations conferring resistance to 1NM-PP1, the genomes of PLK/DUAL, PLK/DUAL res.1, and PLK/DUAL res.2 were sequenced using a 5500xl SOLiD system. Total reads of

A

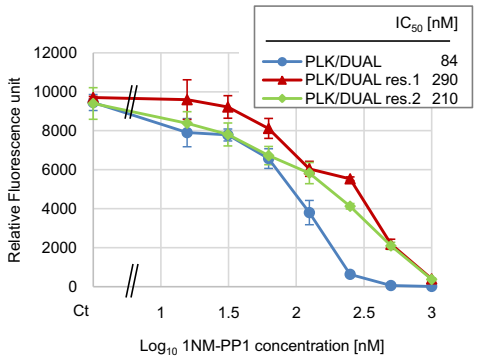

B

clone	Mapped reads	coverage (%)	Average depth
PLK/DUAL	16618344	96.86	20.17
PLK/DUAL res. 1	11514716	96.07	13.98
PLK/DUAL res.2	16263909	97.03	19.74

C

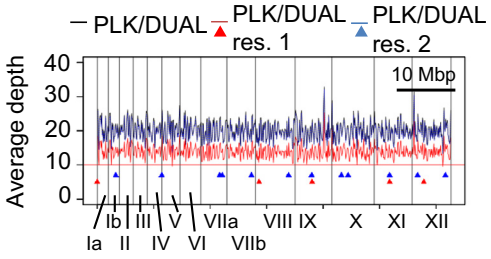

Fig. 1. Establishment of 1NM-PP1 resistant clones and whole-genome sequence. (A) Tachyzoite growth inhibition by 1NM-PP1 was calculated based upon expression of a DsRed Express fluorescent reporter driven by a SAG1 promoter. Cells were cultured for 6 days; fluorescent signals from cell lysates were detected using a fluorimeter, and expressed as relative fluorescent units. Error bars indicate the standard deviations across three independent experiments. IC_{50} values for three clones are inset. (B) Summary of sequence reads that could be aligned to the *T. gondii* genome. (C) Genome-wide average sequence depths of a 100-kbp window from PLK/DUAL (black), PLK/DUAL res.1 (red), and PLK/DUAL res.2 (blue) are plotted. The horizontal red line shows ×10 depth. Scale bar = 10 Mbp. Putative SNVs in PLK/DUAL res.1 (red triangle) and PLK/DUAL res.2 (blue triangle), based on the coding sequence of PLK/DUAL, are plotted.

16,618,344, 11,514,716, and 16,263,909 from PLK/DUAL, PLK/DUAL res.1, and PLK/DUAL res.2, respectively, were mapped to the *T. gondii* ME49 reference genome. Coverage throughout the genome was 97%, 96%, and 97%, respectively (Fig. 1B). The mapped sequence reads showed unbiased coverage and depth throughout the genome (Fig. 1C). Putative SNVs detected in each of the three strains are summarized in Supplemental Table 2. Among them, 5 and 13 SNVs resulting in amino acid substitutions were found in PLK/DUAL res.1 and res.2, respectively (Table 1). Putative SNVs were distributed throughout the genome (Fig. 1C), however both resistant clones contained mutations in gene TGME49_112570 (Table 1).

3.3. Sequence analysis of mutated TgMAPK1

The region surrounding the mutation sites of TGME49_112570 (*T. gondii* mitogen activated protein kinase 1: TgMAPK1) was aligned with HsErk5 and CpCDPK1 to identify the ATP binding site. Structural homology was also used to predict the relationship between TgMAPK1 mutations and their effect on 1NM-PP1 binding (Fig. 2A and Supplemental Fig. 1). PLK/DUAL res.1 contained a Leu 162 to Gln mutation which falls within the protein kinase subdomain III. Superposing the predicted structure of TgMAPK1 on 1NM-PP1-bound CpCDPK1 (PDB: 3NCG) showed that the mutated Leu 162 faced the naphthyl group of 1NM-PP1 (Supplemental Fig. 1). The Ile 171 to Asn mutation in clone PLK/DUAL res.2 mapped to the protein kinase subdomain IV, the putative ATP binding site, and the predicted target of 1NM-PP1.

3.4. Construction of parasites containing a mutated locus in TgMAPK1

To confirm that the mutations in TgMAPK1 were responsible for the resistance to 1NM-PP1, we generated replacement constructs containing a sense mutation in order to include a *Cla*I restriction site to distinguish the inserted construct from the native genomic sequence (Fig. 2B). To determine whether the mutated TgMAPK1 sequence was selected by 1NM-PP1 treatment, plasmids pTgMAPK1_WT, pTgMAPK1_LQ, and pTgMAPK1_IN were nucleofected into WT strain PLK/DUAL and cultured for 3 weeks in the presence of 1000 nM 1NM-PP1, or for 1 week without 1NM-PP1 as a control. Nucleofected control parasites showed no detectable *Cla*I digested bands after 1 week without selection (Supplemental Fig. 2A), indicating a small population possessing homologous recombination at the TgMAPK1 genomic locus. Following selection in the presence of 1000 nM 1NM-PP1, no propagating parasites were obtained from parasites nucleofected with pTgMAPK1_WT, though propagating parasites were obtained from parasites nucleofected with pTgMAPK1_LQ, and pTgMAPK1_IN. PCR-RFLP analysis showed that PCR products generated using genomic DNA from parasites nucleofected with pTgMAPK1_LQ, and pTgMAPK1_IN were readily cleaved by *Cla*I (Supplemental Fig. 2B), confirming that double homologous recombination had occurred in the TgMAPK1 genomic locus. Sequence analysis confirmed the insertion of the *ClaI* and L162Q mutations in 1NM-PP1-selected parasites nucleofected with pTgMAPK1_LQ (Supplemental Fig. 2C upper panels), and the *ClaI* and I171N mutations in 1NM-PP1-selected parasites nucleofected with pTgMAPK1_IN (Supplemental Fig. 2C middle panels).

To identify the mutation that conferred the highest gain of fitness in the presence of 1NM-PP1, the PLK/DUAL parent strain was transfected with a mixture of WT and mutant constructs containing the TgMAPK1 genomic sequences from PLK/DUAL, PLK/DUAL res.1, and PLK/DUAL res.2, followed by selection with 1000 nM 1NM-PP1. Sequence chromatograms from 1NM-PP1 selected parasites showed the presence of a *Cla*I restriction site, consistent with double homologous recombination at the TgMAPK1 genomic locus. Sequence chromatograms of the L162Q mutation

Table 1
Putative missense SNPs detected only in the resistant clones

	Chromosome	SNP position	ref[a]	alt[b]	Gene id	A. A.	ref A.A.	alt A.A.	Gene annotation in ToxoDB [pfam domain search][c]
PLK/DUAL res.1	Ia	416	A	C	TGME49_095210	7	K	T	Hypothetical protein [N/D]
	VIII	655444	C	T	TGME49_030170	1005	S	N	Hypothetical protein [N/D]
	IX	3050049	C	T	TGME49_089070	28	S	L	P-Type cation-transporting ATPase, putative
	XI	2783306	A	T	TGME49_112570	162	L	Q	CMGC kinase, MAPK family (ERK) TgMAPK-1
	XII	2128556	T	A	TGME49_017830	608	I	F	Hypothetical protein [N/D]
PLK/DUAL res.2	Ib	1387776	T	C	TGME49_009660	124	N	D	Hypothetical protein [coiled_coil_region, Telomerase_RBD]
	V	31569	G	C	TGME49_096340	35	R	G	Hypothetical protein [N/D]
	VIIa	3386982	T	C	TGME49_002330	62	D	G	Hypothetical protein [N/D]
	VIIa	3845346	T	A	TGME49_001640	247	E	V	Hypothetical protein [coiled_coil_region]
	VIIb	4408633	T	A	TGME49_056790	550	K	M	Hypothetical protein [ABC_transp_aux]
	VIII	5884619	T	C	TGME49_069330	17	L	P	Hypothetical protein, conserved [coiled_coil_region]
	IX	2981058	A	G	TGME49_088970	97	L	P	Hypothetical protein [N/D]
	X	1737926	A	T	TGME49_026110	424	N	I	Copper-transporting ATPase 1, putative
	X	2927056	A	G	TGME49_024550	296	F	S	Hypothetical protein [N/D]
	XI	2751672	G	T	TGME49_112520	237	H	N	tRNA delta(2)-isopentenylpyrophosphate transferase, putative
XI		2783279	A	T	TGME49_112570	171	I	N	CMGC kinase, MAPK family (ERK) TgMAPK-1
XII		1029418	C	A	TGME49_019220	922	V	F	Hypothetical protein [coiled_coil_region]
XII		5957517	A	T	TGME49_078640	305	V	D	Protein inhibitor of activated STAT protein, putative

Chromosomal positions are shown for the ME49 genome model. N/D, not detected.
[a] Reference bases.
[b] Alternative bases on the positive strand of chromosomes are shown.
[c] For genes annotated as hypothetical proteins in ToxoDB, pfam domain search hits are shown in parentheses.

site showed that the main population of selected parasites contained the L162Q mutation, with only a small population possessing the I171N mutation (Supplemental Fig. 2C lower panels). Selected parasites were cloned by limiting dilution, and the resulting clone containing the TgMAPK1 Leu 162 to Gln mutation was designated PLK/DUAL TgMAPK1^{L162Q}.

Genomic replacement at the loci of TgMAPK1 in chromosome XI was confirmed by PCR followed by cleavage using a restriction enzyme. The TgMAPK1 genomic loci from PLK/DUAL and PLK/DUAL TgMAPK1^{L162Q} were amplified using primers genomeLocusPrimer_F and genomeLocusPrimer_R (Fig. 2B and Supplemental Table 1), resulting in a 16.6-kbp product; *Bam*HI digestion of the PCR products produced fragments approximately 7.8 and 8.8 kbp in length (Fig. 2C). The PCR fragment from PLK/DUAL TgMAPK1^{L162Q} was cut by *Cla*I, resulting in 11- and 5.6-kbp fragments, whereas the PCR fragment from PLK/DUAL was not cut, resulting in a fragment 16.6 kbp in length (Fig. 2C).

PLK/DUAL TgMAPK1^{L162Q} showed an IC_{50} of 300 nM for 1NM-PP1 in tachyzoite growth assays (Fig. 2D). To confirm that resistance was conferred by expression of the mutated TgMAPK1 protein, we transfected a TgMAPK1 overexpression construct (Supplemental Fig. 3A) into PLK/hxgprt-parasites. Established clones were checked for protein expression by Western blotting using an anti-FLAG antibody. Proteins from PLK/TgMAPK1-FLAG and PLK/TgMAPK1^{L162Q}-FLAG showed TgMAPK1-FLAG bands at ~150 kDa (Supplemental Fig. 3B). Bands were slightly higher than the calculated molecular weight of 3xFLAG tagged TgMAPK1 (140 kDa). Protein from the PLK/GFP-FLAG control showed a GFP-FLAG band at approximately 31 kDa. Western blotting with anti-TgALD1 antibody (Sugi et al., 2010) was used to confirm equivalent loading.

PLK/TgMAPK1-FLAG, PLK/TgMAPK1^{L162Q}-FLAG, and PLK/GFP-FLAG were examined by plaque assay with or without 1NM-PP1. PLK/GFP-FLAG showed no plaque at 250 nM 1NM-PP1 (Supplemental Fig. 3C). PLK/TgMAPK1-FLAG showed a small plaque at 250 nM 1NM-PP1 (Supplemental Fig. 3C), while PLK/TgMAPK1^{L162Q}-FLAG showed a medium sized plaque at 250 nM 1NM-PP1 (Supplemental Fig. 3C). These results suggest that overexpression of TgMAPK1 is sufficient to confer modest resistance to 1NM-PP1, while overexpression of TgMAPK1 L162Q confers higher resistance to 1NM-PP1 than WT TgMAPK1 or control GFP expression alone.

3.5. Inhibitory effect of 1NM-PP1 on invasion, egress, and cell division of TgMAPK1 mutant L162Q

Previous reports have demonstrated an inhibitory effect of BKIs on invasion and calcium-induced egress through targeting of TgCDPK1; we therefore examined whether these mechanisms might also be contributing to 1NM-PP1 inhibition of TgMAPK1. 500 nM 1NM-PP1 reduced invasion of PLK/DUAL parasites by >40% relative to untreated controls (Fig. 3A). PLK/DUAL res.1, PLK/DUAL res.2, and PLK/DUAL TgMAPK1^{L162Q} showed similar levels of 1NM-PP1 susceptibility in terms of invasion inhibition, with no significant differences observed.

Calcium-induced egress was also examined. Parasites were treated with A23187, a calcium ionophore that causes increased Ca^{2+} concentration in parasites leading to egress of parasites from infected cells, with or without 1NM-PP1. All constructs (PLK/DUAL, PLK/DUAL res.1, PLK/DUAL res.2, and PLK/DUAL TgMAPK1^{L162Q}) showed a similar decrease in A23187-induced egress. Egress rates were approximately 80% for all constructs in the absence of drug; this rate dropped to <20% upon addition of 250 nM 1NM-PP1 (Fig. 3B).

As a final step we examined tachyzoite cell division. At 12 h, the average numbers of parasites per vacuole of PLK/DUAL, PLK/DUAL res.1, PLK/DUAL res.2, and PLK/DUAL TgMAPK1^{L162Q} were 1.58, 1.61, 1.60, and 1.60 without 1NM-PP1 treatment and 1.31, 1.53, 1.43, and 1.54 with 250 nM 1NM-PP1 treatment, respectively (Fig. 4A). At 24 h the average numbers of parasites per vacuole of PLK/DUAL, PLK/DUAL res.1, PLK/DUAL res.2, and PLK/DUAL TgMAPK1^{L162Q} were 4.85, 4.83, 4.62 and 4.81 without 1NM-PP1 treatment and 3.53, 4.38, 4.33, and 4.56 with 250 nM 1NM-PP1 treatment, respectively (Fig. 4A). These results demonstrate a significant change in parasite numbers between the WT PLK/DUAL strain and resistant clones in the presence of 250 nM 1NM-PP1 at both 12 and 24 h (Fig. 4A), suggesting that TgMAPK1 mutational resistance to 1NM-PP1 is mediated through cell division regulation in drug susceptibility.

3.6. Effect of TgMAPK1 mutations on susceptibility to other BKIs

TgMAPK1 mutants L162Q and I171N were next examined for cross resistance to other BKIs. 3BrB-PP1 inhibited clones PLK/DUAL, PLK/DUAL res.1, PLK/DUAL res.2, and PLK/DUAL TgMAPK1^{L162Q} at IC_{50} values of 41, 81, 30 and 95 nM, respectively

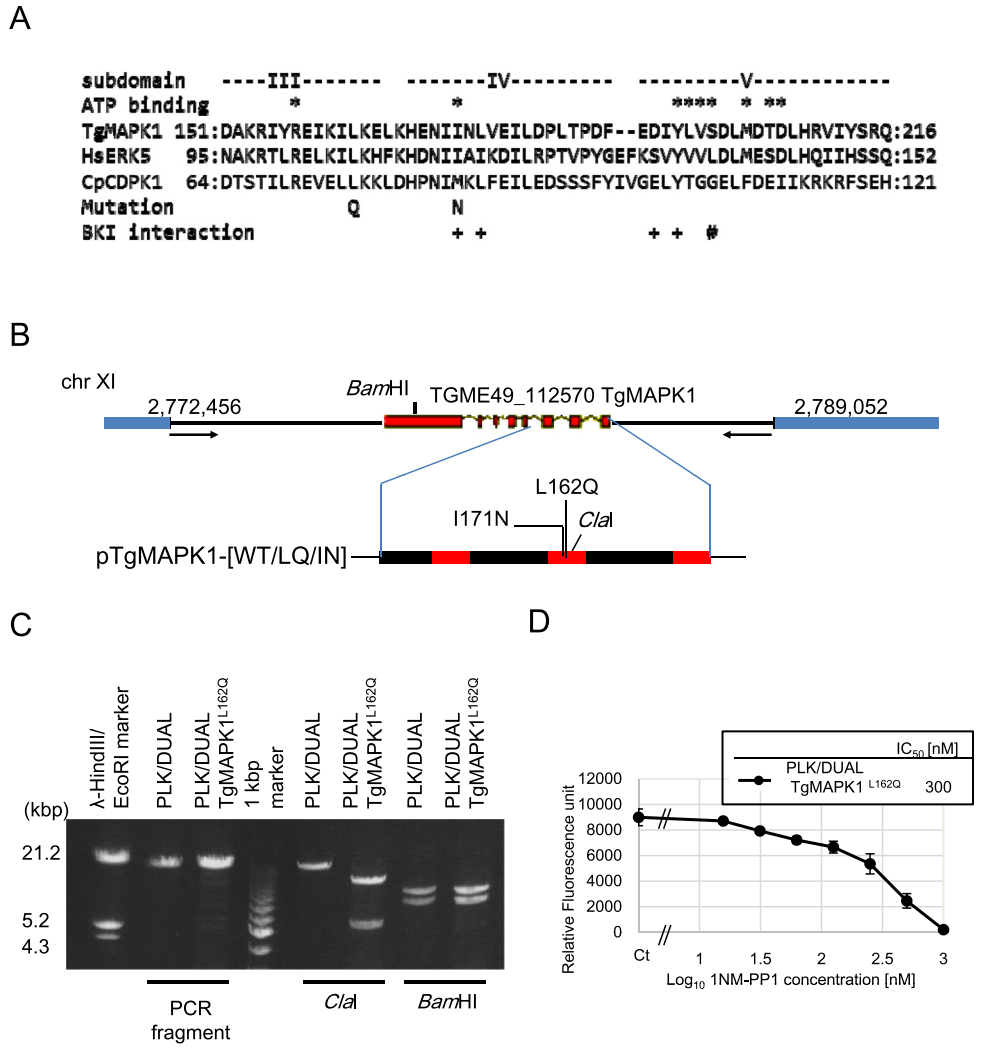

Fig. 2. 1NM-PP1 selects for mutations in TgMAPK1. (A) Alignment of the mutated region of TgMAPK1 with proteins HsErk5 and CpCDPK1. '∗' indicates the ATP-binding amino acid position, '+' indicates the 1NM-PP1 bound amino acid position in CpCDPK1, and '#' indicates the position of the gatekeeper residue. (B) Schematic depicting the chromosomal DNA around TGME49_112570 and a replacement construct. The blue boxes show coding sequences for genes TGME49_112560 and TGME49_112580. The red box shows the TGME49_112570 exon on the negative strand of chromosome XI. Arrows represent primers genomeLocusPrimer_F and genomeLocusPrimer_R used in PCR-RFLP analysis. A *Cla*I restriction site is contained in all plasmids; mutations L162Q and I171N are encoded by plasmids pTgMAPK1_LQ and pTgMAPK1_IN, respectively. (C) PCR fragments of chromosome XI 2,772,456–2,789,052 from PLK/DUAL and PLK/DUAL TgMAPK1^{L162Q} were cut with *Cla*I or *Bam*HI and separated by 0.7% agarose gel electrophoresis. (D) Tachyzoite growth inhibition by 1NM-PP1 was determined by measuring DsRed Express fluorescent reporter expression. Cells were cultured for 6 days; fluorescent signals in cell lysates were detected using a fluorimeter, and expressed as relative fluorescent units. Error bars indicate the standard deviations across three independent experiments. IC_{50} values are inset.

(Supplemental Fig. 4A). Inhibitor 3MB-PP1 elicited a similar pattern of sensitivity, with IC_{50} values for PLK/DUAL, PLK/DUAL res.1, PLK/DUAL res.2, and PLK/DUAL TgMAPK1^{L162Q} of 73, 146, 90 and 176 nM, respectively (Supplemental Fig. 4B). Parasite clones harboring the L162Q mutation showed consistently higher IC_{50} values for both 3BrB-PP1 and 3MB-PP1 compared to the parental strain PLK/DUAL. On the other hand, parasite clones expressing the I171N mutation (PLK/DUAL res.2) showed similar IC_{50} value to 3BrB-PP1 and 3MB-PP1 as PLK/DUAL, demonstrating selective resistance to BKI 1NM-PP1.

4. Discussion

In *T. gondii*, the main target of 1NM-PP1 is TgCDPK1 (Lourido et al., 2010; Ojo et al., 2010; Sugi et al., 2010; Larson et al., 2012). This report represents the first description of mutations in TgMAPK1 capable of conferring resistance to 1NM-PP1. Mutants were generated using random mutagenesis followed by whole-genome sequencing. Considering the hundreds of SNVs detected by whole-genome sequencing, a lower concentration of ENU may be sufficient for whole genome mutagenesis. By decreasing the number of SNVs in a given sequence, identification of the mutation responsible for a desired phenotype becomes much easier. Surprisingly neither resistant clone had mutations in TgCDPK1. As this study failed to identify the known target of 1NM-PP1, higher concentration of ENU or larger starting parasites number may be useful for developing more robust target identification.

The method we chose for generating resistant clones in this study was somewhat slower than the usual selection time of 3 days to 1 week using the standard selectable marker HXGPRT to isolate transgenic parasites. Instead we selected for 3 weeks (three

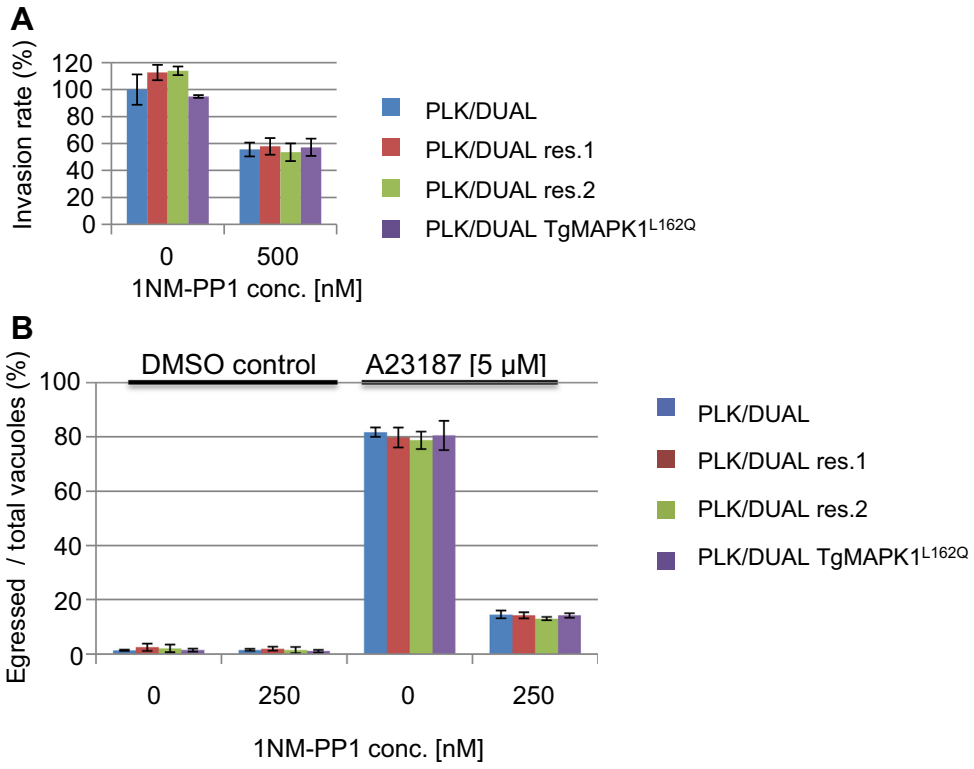

Fig. 3. Parental PLK/DUAL and resistant clones had comparable susceptibility to 1NM-PP1 at invasion and calcium-induced egress. (A) Parasites were allowed to invade for 30 min in the presence of 500 nM 1NM-PP1 or control solvent DMSO. Extracellular parasites were stained with anti-SAG1 antibodies. Invasion rate was determined by comparing the number of invaded parasites to total parasite counts. Invasion rates are reported as percentages relative to that of untreated PLK/DUAL parasites. More than 200 parasites were counted in each test. (B) The egress rate denotes the number of egressed vacuoles per total number of vacuoles as percentages. Calcium signal stimulation was performed using 5 µM A23187 for 5 min with or without 250 nM 1NM-PP1. More than 200 vacuoles were counted in each test. (A and B) Error bars indicate standard deviations across three independent experiments; statistical evaluations were performed using Student's *t*-test comparing PLK/DUAL and resistant parasite strains.

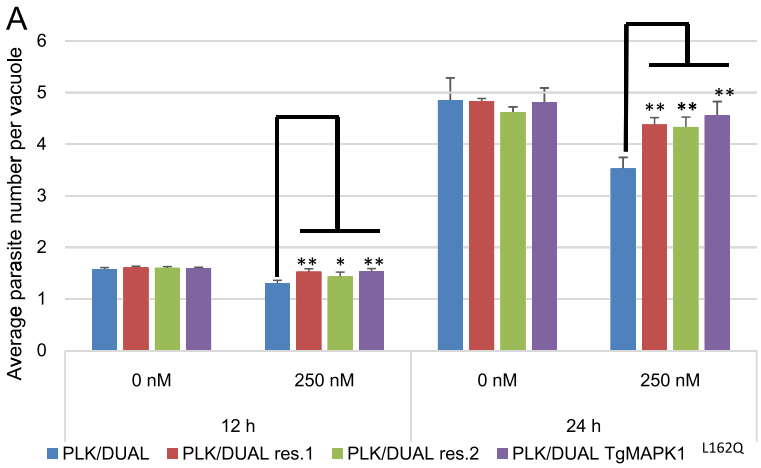

Fig. 4. Tachyzoite cell division rates of resistant clones were not decreased in the presence of 1NM-PP1. (A) Average parasite number per vacuole after 12 and 24 h incubation, with or without 250 nM 1NM-PP1, is shown. More than 200 vacuoles were counted in each test. Error bars indicate standard deviations across three independent experiments; statistical evaluations were performed using Student's *t*-test comparing PLK/DUAL and resistant parasites. '∗' denotes $p < 0.05$; '∗∗' denotes $p < 0.01$

passages) to screen for resistant parasites. However, after screening, parasites were cloned and propagated in the absence of selection pressure, meaning the time necessary to establish clones after the screening was almost the same as with standard transgenic parasites.

The resistant clones did not demonstrate resistance to 1NM-PP1 at invasion or egress where TgCDPK1 has been shown to play an important role (Lourido et al., 2010). Instead, resistance was mediated through altered susceptibility during cell division. This alternative pattern of resistance may not be achieved through complementation of TgCDPK1 function directly, but instead by rescuing a different inhibitory effect of 1NM-PP1 on cell division which had not previously been evaluated. Considering that TgMAPK1 has been shown to function in stress responses (Brmlik et al., 2011), inhibition of TgMAPK1 could affect the parasite's ability to respond to different stresses caused by 1NM-PP1, including TgCDPK1 inhibition.

The PLK/DUAL reporter strain is an excellent system for measuring bradyzoite differentiation using a fluorescent reporter (Unno et al., 2009). Our resistant clones and BKIs may represent a valuable tool to study the function of TgMAPK1 in bradyzoite differentiation.

The tachyzoite cell cycle is regulated by several protein kinase signals, including a PKA signal inhibited by a cAMP analog (Eaton et al., 2006), PKA specific inhibitors (Kurokawa et al., 2011), TgNEK1 (Gubbels et al., 2008), TPK2 (Khan et al., 2002), and a MAPK signal inhibited by p38 MAPK inhibitors (Wei et al., 2002). Analysis of the *T. gondii* genome suggests that the MAPK signaling cascade lacks the canonical upstream protein kinase STE group (Miranda-Saavedra et al., 2012). While its role in the cell cycle is not yet clear, TgMAPK1 may interact with the protein kinase signals described above instead of STE.

Among the putative SNVs detected, both resistant clones had a mutation in TgMAPK1. PLK/DUAL res.2 carried a mutation at the predicted ATP and 1NM-PP1 binding site (Ile171). Protein kinase activity may be altered by this mutation; however, no significant change in tachyzoite growth was observed in the absence of 1NM-PP1. Furthermore, the mutated site in PLK/DUAL res.1 (Leu162) was predicted to face the nonpolar naphthyl group of 1NM-PP1 (Supplemental Fig. 1). The polar characteristics of Gln 162 in these resistant parasites might disrupt the nonpolar interaction, decreasing the affinity between 1NM-PP1 and TgMAPK1.

Generation of the active recombinant enzyme will be necessary for *in vitro* kinase assays. *In vitro* assays will allow for detailed analyses of protein kinase activity in the presence of inhibitors such as 1NM-PP1, as well as the effect of mutations on enzyme activity. Preliminary efforts to isolate the active form of TgMAPK1 were unsuccessful. A truncated isoform of TgMAPK1 containing the entire protein kinase domain (GenBank ID: AY684849) fused with the maltose binding protein or glutathione S transferase was expressed in *Escherichia coli* or using a baculovirus system; however, the resulting protein did not exhibit sufficient enzymatic activity for use in drug inhibition assays (data not shown). One possible explanation for this deficiency may be tied to enzyme regulation. MAPKs from other species require activation by corresponding MAPKKs for full enzyme activity. Identification of protein kinases which can activate TgMAPK1 may therefore be necessary.

The full length isoform of TgMAPK1, which is predicted by both RNA-seq and gene modeling data in ToxoDB, alters the susceptibility of parasites to 1NM-PP1 when expressed in parasites, suggesting that this isoform may contribute to kinase activity. Attempts at expressing the full-length TgMAPK1 isoform in *E. coli* were also unsuccessful; an alternative system suitable for the expression of large proteins will therefore be needed.

Parasite clones expressing an L162Q mutation in TgMAPK1 exhibited cross resistance to other BKIs (3BrB-PP1 and 3MB-PP1), suggesting a more universal role for TgMAPK1 in BKI resistance. The possibility of mutations beyond TgCDPK1 should therefore be considered when BKI resistance is observed. Alternatively, clones possessing the I171N mutation in TgMAPK1 (PLK/DUAL res.2) showed similar susceptibilities to 3MB-PP1, along with slightly higher susceptibilities to 3BrB-PP1. The specificity of this mutation to 1NM-PP1 suggests structural differences between this and other BKIs, which may provide insight into the activity of this compound.

BKI derivatives with enhanced activity against TgCDPK1 have been reported recently (Larson et al., 2012). This activity is mediated through substitutions at the R2 position of the PP-based inhibitor. TgMAPK1 mutations described here aligned to the naphthyl group at the R1 position (Supplemental Fig. 1). Resistant clones in the present report may not be cross resistant to R2 substituted derivatives; however, use of resistant parasite clones is necessary to predict the occurrence of BKI resistance in *T. gondii*.

The mutation in TgMAPK1 conferring resistance to 1NM-PP1 did not occur at the gatekeeper residue, suggesting the likelihood of similar mutations that may confer resistance in other analog sensitive kinases. Genome-wide screening these and other non-gatekeeper mutation conferring resistance to BKIs is therefore warranted. This work demonstrates the usefulness of random mutagenesis followed by whole-genome sequencing for the screening of such mutations.

Acknowledgments

PLK/DUAL parasites were gratefully given by Dr. Takashima (Gifu, Univ). PLK/HXGPRT- was obtained through the NIH AIDS Reagent Program, Division of AIDS, NIAID, NIH from Dr. David Roos. Molecular graphics images were produced using the UCSF Chimera package from the Computer Graphics Laboratory, University of California, San Francisco (supported by NIH P41 RR-01081). This study was supported by a JSPS Research Fellowship for Young Scientists, Grant-in-Aids for Young Scientists, Exploratory Research, Scientific Research on Innovative Areas (3308) from the Ministry of Education, Culture, Science, Sports, and Technology (MEXT) of Japan, Bio-oriented Technology Research Advancement Institution (BRAIN), and Program to Disseminate Tenure Tracking System from Japan Science and Technology Agency (JST).

Appendix A. Supplementary data

Supplementary data associated with this article can be found, in the online version, at http://dx.doi.org/10.1016/j.ijpddr.2013.04.001.

References

Arnold, K., Bordoli, L., Kopp, J., Schwede, T., 2006. The SWISS-MODEL workspace: a web-based environment for protein structure homology modelling. Bioinformatics 22, 195–201.

Arrizabalaga, G., Ruiz, F., Moreno, S., Boothroyd, J.C., 2004. Ionophore-resistant mutant of *Toxoplasma gondii* reveals involvement of a sodium/hydrogen exchanger in calcium regulation. J. Cell Biol. 165, 653–662.

Brmlik, M.J., Pandeswara, S., Ludwig, S.M., Murthy, K., Curiel, T.J., 2011. Parasite mitogen-activated protein kinases as drug discovery targets to treat human protozoan pathogens. J. Signal. Transduct. 2011, 971968.

Eaton, M., Weiss, L., Kim, K., 2006. Cyclic nucleotide kinases and tachyzoite–bradyzoite transition in *Toxoplasma gondii*. Int. J. Parasitol. 36, 107–114.

Farrell, A., Thirugnanam, S., Lorestani, A., Dvorin, J.D., Eidell, K.P., Ferguson, D.J., Anderson-White, B.R., Duraisingh, M.T., Marth, G.T., Gubbels, M.J., 2012. A DOC2 protein identified by mutational profiling is essential for apicomplexan parasite exocytosis. Science 335, 218–221.

Gubbels, M.J., Lehmann, M., Muthalagi, M., Jerome, M.E., Brooks, C.F., Szatanek, T., Flynn, J., Parrot, B., Radke, J., Striepen, B., White, M.W., 2008. Forward genetic analysis of the apicomplexan cell division cycle in *Toxoplasma gondii*. PLoS Pathog. 4, e36.

Hanks, S.K., Hunter, T., 1995. Protein kinases 6. The eukaryotic protein kinase superfamily: kinase (catalytic) domain structure and classification. FASEB J. 9, 576–596.

Khan, F., Tang, J.Z., Qin, C.L., Kim, K., 2002. Cyclin-dependent kinase TPK2 is a critical cell cycle regulator in *Toxoplasma gondii*. Mol. Microbiol. 45, 321–332.

Kurokawa, H., Kato, K., Iwanaga, T., Sugi, T., Sudo, A., Kobayashi, K., Gong, H., Takemae, H., Recuenco, F.C., Horimoto, T., Akashi, H., 2011. Identification of *Toxoplasma gondii* cAMP dependent protein kinase and its role in the tachyzoite growth. PLoS ONE 6, e22492.

Larson, E.T., Ojo, K.K., Murphy, R.C., Johnson, S.M., Zhang, Z., Kim, J.E., Leibly, D.J., Fox, A.M., Reid, M.C., Dale, E.J., Perera, B.G., Kim, J., Hewitt, S.N., Hol, W.G., Verlinde, C.L., Fan, E., Van Voorhis, W.C., Maly, D.J., Merritt, E.A., 2012. Multiple determinants for selective inhibition of apicomplexan calcium-dependent protein kinase CDPK1. J. Med. Chem. 55, 2803–2810.

Li, H., Handsaker, B., Wysoker, A., Fennell, T., Ruan, J., Homer, N., Marth, G., Abecasis, G., Durbin, R., Subgroup, G.P.D.P., 2009. The sequence alignment/map format and SAMtools. Bioinformatics 25, 2078–2079.

Lourido, S., Shuman, J., Zhang, C., Shokat, K.M., Hui, R., Sibley, L.D., 2010. Calcium-dependent protein kinase 1 is an essential regulator of exocytosis in *Toxoplasma*. Nature 465, 359–362.

Marchler-Bauer, A., Lu, S., Anderson, J.B., Chitsaz, F., Derbyshire, M.K., DeWeese-Scott, C., Fong, J.H., Geer, L.Y., Geer, R.C., Gonzales, N.R., Gwadz, M., Hurwitz, D.I., Jackson, J.D., Ke, Z., Lanczycki, C.J., Lu, F., Marchler, G.H., Mullokandov, M., Omelchenko, M.V., Robertson, C.L., Song, J.S., Thanki, N., Yamashita, R.A., Zhang, D., Zhang, N., Zheng, C., Bryant, S.H., 2011. CDD: a conserved domain database for the functional annotation of proteins. Nucleic Acids Res. 39, D225–229.

Miranda-Saavedra, D., Gabaldón, T., Barton, G.J., Langsley, G., Doerig, C., 2012. The kinomes of apicomplexan parasites. Microbes Infect. 14, 796–810.

Murphy, R.C., Ojo, K.K., Larson, E.T., Castellanos-Gonzalez, A., Perera, B.G., Keyloun, K.R., Kim, J.E., Bhandari, J.G., Muller, N.R., Verlinde, C.L., White Jr., A.C., Merritt, E.A., Van Voorhis, W.C., Maly, D.J., 2010. Discovery of potent and selective inhibitors of calcium-dependent protein kinase 1 (CDPK1) from *C. parvum* and *T. gondii*. ACS Med. Chem. Lett. 1, 331–335.

Nagamune, K., Moreno, S.N., Sibley, L.D., 2007. Artemisinin-resistant mutants of *Toxoplasma gondii* have altered calcium homeostasis. Antimicrob. Agents Chemother. 51, 3816–3823.

Ojo, K., Larson, E., Keyloun, K., Castaneda, L., Derocher, A., Inampudi, K., Kim, J., Arakaki, T., Murphy, R., Zhang, L., Napuli, A., Maly, D., Verlinde, C., Buckner, F., Parsons, M., Hol, W., Merritt, E., Van Voorhis, W., 2010. *Toxoplasma gondii* calcium-dependent protein kinase 1 is a target for selective kinase inhibitors. Nat. Struct. Mol. Biol. 17, 602–607.

Ojo, K.K., Pfander, C., Mueller, N.R., Burstroem, C., Larson, E.T., Bryan, C.M., Fox, A.M., Reid, M.C., Johnson, S.M., Murphy, R.C., Kennedy, M., Mann, H., Leibly, D.J., Hewitt, S.N., Verlinde, C.L., Kappe, S., Merritt, E.A., Maly, D.J., Billker, O., Van Voorhis, W.C., 2012. Transmission of malaria to mosquitoes blocked by bumped kinase inhibitors. J. Clin. Invest. 122, 2301–2305.

Pettersen, E.F., Goddard, T.D., Huang, C.C., Couch, G.S., Greenblatt, D.M., Meng, E.C., Ferrin, T.E., 2004. UCSF chimera – a visualization system for exploratory research and analysis. J. Comput. Chem. 25, 1605–1612.

Ray, A., Cowan-Jacob, S.W., Manley, P.W., Mestan, J., Griffin, J.D., 2007. Identification of BCR-ABL point mutations conferring resistance to the Abl kinase inhibitor AMN107 (nilotinib) by a random mutagenesis study. Blood 109, 5011–5015.

Roos, D.S., Donald, R.G.K., Morrissette, N.S., Moulton, A.L.C., 1994. Molecular tools for genetic dissection of the protozoan parasite Toxoplasma gondii. Meth. Cell Biol. 45, 27–63.

Shokat, K., Velleca, M., 2002. Novel chemical genetic approaches to the discovery of signal transduction inhibitors. Drug Discov. Today 7, 872–879.

Sugi, T., Kato, K., Kobayashi, K., Watanabe, S., Kurokawa, H., Gong, H., Pandey, K., Takemae, H., Akashi, H., 2010. Use of the kinase inhibitor analog 1NM-PP1 reveals a role for *Toxoplasma gondii* CDPK1 in the invasion step. Eukaryot. Cell 9, 667–670.

Unno, A., Suzuki, K., Batanova, T., Cha, S., Jang, H., Kitoh, K., Takashima, Y., 2009. Visualization of *Toxoplasma gondii* stage conversion by expression of stage-specific dual fluorescent proteins. Parasitology 136, 579–588.

Wei, S., Marches, F., Daniel, B., Sonda, S., Heidenreich, K., Curiel, T., 2002. Pyridinylimidazole p38 mitogen-activated protein kinase inhibitors block intracellular *Toxoplasma gondii* replication. Int. J. Parasitol. 32, 969–977.

Weisberg, E., Griffin, J.D., 2000. Mechanism of resistance to the ABL tyrosine kinase inhibitor STI571 in BCR/ABL-transformed hematopoietic cell lines. Blood 95, 3498–3505.